A SIMPLE MODEL TO ESTIMATE ELECTRICAL DECAY TIMES IN ANVIL CLOUDS

J.C. Willett[1] and J.E. Dye[2]

[1]P.O. Box 41, Garrett Park, MD 20896, USA
[2]NCAR/MMM, P.O. Box 3000, Boulder, CO 87307, USA

ABSTRACT: A model is developed that uses measured particle-size distributions to show that pre-existing electrification can persist for well over an hour in realistic anvil clouds if the initial electric-field intensities are high enough.

INTRODUCTION

Thunderstorm anvil clouds are a cause for concern to the space-launch community because they are known occasionally to be strongly electrified and because they are suspected to be capable of storing charge for long periods of time [*e.g.*, Marshall et al., 1989]. Therefore, during 2000 and 2001 an experiment was conducted in the vicinity of the NASA Kennedy Space Center, Florida, to measure both the ambient electrostatic fields and the size/shape distributions of the cloud and precipitation particles in anvils [Dye, *et al.*, 2002]. The purpose of the present modeling is to predict the time required for the decay of electrification within such clouds from the measured microphysical properties. The decay modeled here is that caused by electrical conduction currents flowing in the reduced conductivity within these clouds. A companion paper [Dye, *et al.*, this conference] discusses these predictions in relation to the observed radar, electrical, and microphysical structure of the same clouds.

MODEL DESCRIPTION

Based on a suggestion by Paul Krehbiel [NASA/USAF Lightning Advisory Panel (LAP) meeting, Tucson, AZ, January, 1998], a simple model has been developed to calculate the temporal decay of the vertical electric field, $E(t)$, within a previously charged, horizontally stratified anvil cloud, given a measured particle-size distribution, $N(d)$. This model envisions a microphysically uniform and constant, motionless cloud that contains a thin layer of positive charge between two thin, negative screening layers. (For simplicity each screening layer is assumed to contain half the charge area density of the internal positive layer.) The positive and negative ions within this cloud are assumed to have equal concentrations and identical properties. Because of the simple geometry, all variables are uniform in magnitude throughout the bulk of the cloud (between the charge layers), so the volume charge density there remains zero. Thus,

$$\mathrm{d}E/\mathrm{d}t = -J(t)/\varepsilon_0 = -2ekn(t)E(t)/\varepsilon_0 \qquad (1)$$

where $J(t)$ is the vertical conduction-current density, e is the electronic charge, k is the small-ion mobility, $n(t)$ is the polar small-ion density, and ε_0 is the dielectric permittivity of free space. (The sign convention is such that the vertical vector components, E and J, are positive above the internal positive layer and negative below it.) Krehbiel [1967] had shown that $J(t)$ becomes constant -- independent of both k and $E(t)$ -- when the electric field is strong enough. In this limit the field decay is linear and can be quite slow.

Our analysis begins with the steady-state, small-ion budget equation in a population of stationary, mono-disperse, spherical cloud particles, from Pruppacher and Klett [1978, Eq. 17-40]. After neglect of small-ion recombination and aerosol attachment, simplification to uncharged cloud particles, generalization to allow non-spherical shapes, and use of the "Einstein relation" [*e.g.*, Pruppacher and Klett, 1978, Eq. 12-21], this equation becomes,

$$q \approx A_e(d)kN(d)n(t)E(t) + [C(d)/\varepsilon_0][kKT/e]N(d)n(t) \qquad (2)$$

where q is the ionization rate, $A_e(d)$ is the effective electrical cross section of a particle of long dimension, d, $C(d)$ is the electrical capacitance of that particle, K is Boltzmann's constant, and T is absolute temperature. The first term on the right represents the small-ion loss rate due to field-driven attachment of ions to cloud particles, which dominates at high enough electric-field intensity, producing an ion density that is inversely proportional to field. The second term is the diffusive loss rate, which dominates at low fields, resulting in an Ohmic conductivity, independent of E. When $N(d)$ is a particle-size spectrum, each term on the right-hand side of (2) must be regarded as an integral over the size distribution.

Equation 2 can be solved for $n(t)$ and inserted into (1) to give a first-order, non-linear differential equation for $\mathrm{d}E/\mathrm{d}t$:

$$\mathrm{d}E/\mathrm{d}t = -2eq\{\varepsilon_0 N(d)[A_e(d) + C(d)KT/(\varepsilon_0 eE(t))]\}^{-1} \qquad (3)$$

where again each term in the denominator on the right is to be considered an integral over the size distribution. Notice that, although both loss terms in (2) depend on the small-ion mobility, (3) is independent of k; thus no results below (except those in Figure 2 itself) depend on k. This equation has been solved numerically to obtain $E(t)$ for various observed particle-size spectra. In general A_e and C are functions of the shape, as well as the long dimension, of the cloud particles. For all numerical calculations herein, however, we have approximated particles of all sizes by spheres of diameter, d. Thus, $A_e(d) = 3\pi d^2/4$ and $C(d) = 2\pi\varepsilon_0 d$. This turns out to be the conservative approach, as it predicts the slowest possible electrical decay for a given size distribution.

RESULTS

Here we present one example of this numerical solution for a dense anvil cloud that was penetrated at 210800 UT on 13 June 2000 at a flight altitude of 10.5 km. This case was chosen for illustration because it is typical of the high particle concentrations, field intensities, and radar returns that were encountered at the windward ends of well-developed anvils, just downstream from the convective cores of their parent thunderstorms. (The spatial and temporal structure of this same anvil are discussed in detail by Dye, *et al.* [this conference].) Figure 1 gives the measured size distribution -- a composite of data from the FSSP, 2-DC, and HVPS instruments [Dye, *et al.*, 2002] -- integrated over about 3.5 km of flight track. From this $N(d)$ it is easy to calculate size spectra of the small-ion loss rates that are represented by the two terms on the right-hand side of Equation 2. Per unit small-ion density -- that is, with $n(t)$ cancelled out -- the field-driven-attachment rate is shown in black and the diffusive-loss rate is shown in gray in Figure 2, where we have taken $k = 3.6 \text{ X } 10^{-4}$ $m^2/(Vs)$ and $T = 225$ K. To compute the former rate, it is necessary to assume an electric-field intensity. For that purpose we have computed the "transition field," E_γ, at which the two loss rates, integrated over particle size, are equal -- 551 V/m in this case. (The only effect of changing the ambient field is to shift the black curve vertically in proportion to E.) In plotting the figure, each of these loss terms has been multiplied by the particle size, d, to compensate for the effect of the logarithmic horizontal axis. This weighting is convenient because larger magnitudes on the graph make larger contributions to the total ion-loss rate (the integral over particle size).

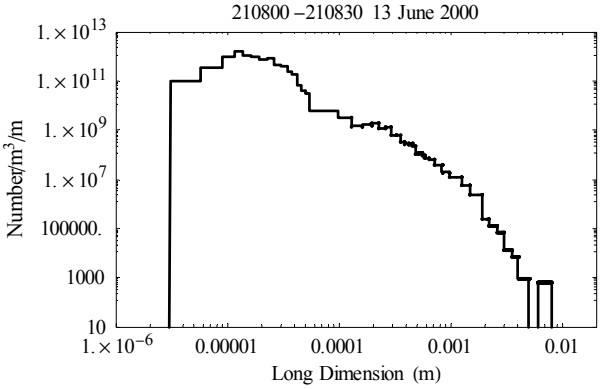

Figure 1 -- Composite particle-size distribution integrated over 30 s of flight time (3.5 km of distance).

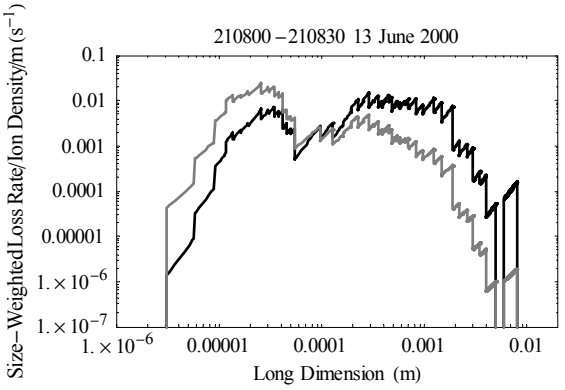

Figure 2 -- Weighted small-ion loss rates from electrical (black) and diffusive (gray) attachment.

Two conclusions are immediately evident from Figure 2. First, the small particles (in the 10 - 50 μm size range) dominate the diffusive loss, dependent as it is on particle diameter through C, whereas the electrical-attachment loss is dominated by the intermediate size particles (0.2 - 2 mm in diameter) because of the dependence of A_e on d^2. Second, in spite of the logarithmic vertical axis (which spoils the equal-areas attribute of the d-weighting in Figure 2) it is obvious that the integrated electrical-attachment loss will dominate the integrated diffusive loss at field intensities much greater than E_γ. Because of the similarities in shape among measured size distributions from the dense anvils in our data set [Dye, *et al.*, this conference], both of these conclusions are generally valid.

Solution of Equation 3 (after the implied integration over the size distribution in Figure 1) results in the field decay that is shown in Figure 3 (black curve), where the initial condition was $E(0) = 50$ kV/m and we have taken $q = 3.2 \text{ X } 10^7$ pairs/(m^3s) -- primarily due to cosmic radiation at anvil altitudes. Evidently the decay is linear at high fields, as pointed out by Krehbiel [LAP meeting, Tucson, AZ, January, 1998]. The behavior at low fields is shown on expanded scales in Figure 4 (black curve), where the decay can be seen to become approximately exponential as diffusion becomes the dominant ion-loss mechanism. The gray line in both figures is an extrapolation of the initial linear decay to zero field, yielding an estimated electrical-decay time --

the intercept at $E(\tau_E) \equiv 0$ -- of $\tau_E = 6054$ s (more than 1½ hours!). The considerable separation between the black and gray traces in Figure 4 is a manifestation of the breadth of the particle-size distribution in Figure 1: As may be inferred from Figure 2, the smallest particles change over from predominantly field-driven attachment to predominantly diffusive attachment of small ions at intermediate fields (~10 kV/m), whereas the very largest particles do not change over until low fields (a few times 10 V/m).

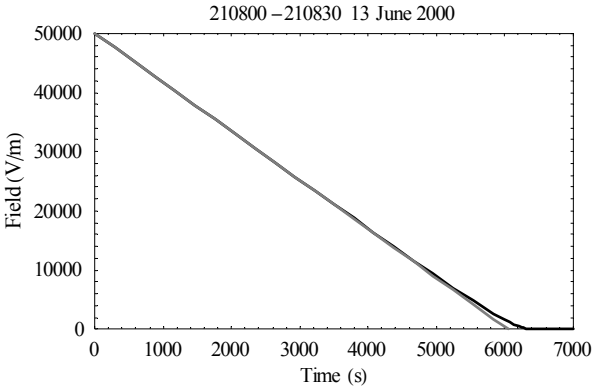

Figure 3 -- Electric-field decay from 50 kV/m. Numerical solution of Eq. 3 (black). Extrapolation of initial linear slope (gray) overlays it at high fields.

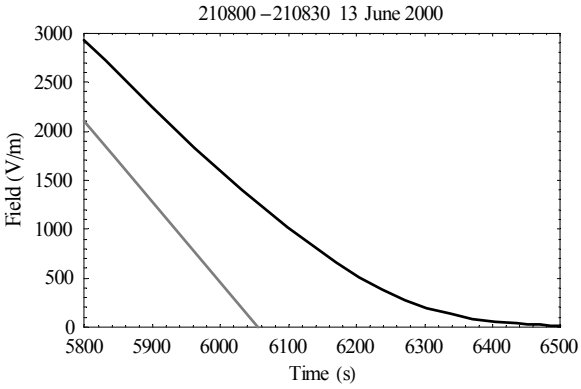

Figure 4 -- Enlargement of final decay shown in Fig.3 (black). Extrapolation of initial linear slope (gray) diverges significantly at moderate fields.

LIMITING BEHAVIOR

Next we examine the limiting behavior of this simple model at high and low field intensities. For any individual particle size, d, the condition for equal field-driven and diffusive ion-loss rates in Equation 2 can be identified by a value of unity for the dimensionless ratio, $\gamma \equiv A_e e \varepsilon_0 E/(CKT)$, which is essentially the same as Equation 5 of *Klett* [1971]. When $\gamma \gg 1$, we are in the "high-field limit," which is of most interest here. Solving (2) for the small-ion density in this limit, we find $n(t) \approx q/[A_e k N E(t)]$. Thus, the conduction-current density in (1) takes on a constant value that is determined only by cloud properties,

$$J(t) \approx J_0 \equiv 2eq/(A_e N), \quad E(t) >> E_\gamma \tag{4}$$

as shown previously by Krehbiel [1967]. This happens because small ions are being "swept out" by electrical attachment to cloud particles at a rate proportional to their drift velocity in the electric field. Solving (1) then yields linear field decay,

$$E(t) = E_0 - J_0 t/\varepsilon_0, \quad E(t) >> E_\gamma \tag{5}$$

where E_0 is an assumed initial field intensity. Thus an "electrical-decay time scale" can be defined as $\tau_E \equiv \varepsilon_0 E_0/J_0 = E_0 A_e \varepsilon_0 N/(2eq)$, essentially that determined with respect to Figure 3 above. When $\gamma \ll 1$, on the other hand, we are in the "low-field limit." This limit results in exponential decay of $E(t)$ with a "diffusive relaxation time," $\tau_D \equiv CKTN/(2e^2 q)$. Obviously each of these time scales can be generalized to any given size distribution $[N(d), A_e(d), C(d)]$ by integrating the corresponding loss rate over d. (Because of the form of $A_e(d)$ for spheres, we see that τ_E is directly proportional to the total cross-section area of cloud particles per unit volume.) The two limits are separated by the condition, $\gamma(E_\gamma) \equiv 1$, which can be solved for the transition field, $E_\gamma = CKT/(A_e e \varepsilon_0)$. (The general definition of E_γ was given earlier in terms of the two integrated loss rates.) τ_E is only meaningful when the field intensities of interest are much larger than E_γ, and neither of these times scales is valid unless it is much larger than the electrical relaxation time in clear air -- roughly 20 s at 10 km altitude.

From only the measured particle-size spectrum (either assuming spherical shape, as done here, or using an observed dependence of particle shape on size), absolute temperature, and flight altitude (from which the ambient ionization rate is estimated), it is possible to compute τ_E, E_γ, and τ_D versus time during anvil-cloud penetrations. In the case analyzed in detail above, for example, $\tau_E = 5963$ s, $E_\gamma = 551$ V/m, and $\tau_D = 66$ s. (The minor difference from the previous value of τ_E results from the numerical-extrapolation method that was used in Figure 3.) The results of such calculations are compared with other data from the experiment by Dye, *et al*. [this conference].

A LIMITED GENERALIZATION

Equation 1 suggests that the present model might apply only to a single, very specialized geometry -- strict horizontal homogeneity of the cloud and its charge distribution. Since Equation 2 (which represents the cloud microphysics) makes no reference to geometry, however, the applicability of the model can be extended somewhat, as follows. Consider a spherically symmetric cloud with a compact, positive, initial charge, Q_0, embedded at its center, $r = 0$, and surrounded by a negative screening layer. (We continue to assume uniform, constant microphysics throughout this cloud.) In this geometry all vectors are radial instead of vertical, as indicated by the subscript, r, on the only non-zero components of field and current density. Although the field intensity is no longer uniform throughout the cloud, the current density everywhere inside the screening layer remains a constant, $J_r(r,t) = J_0$, as defined in (4), as long as $E_r(r,t) >> E_\gamma$, which transition field also remains as defined above. The main difference from the horizontally homogeneous case is that the initially uncharged bulk of the cloud accumulates a non-uniform volume charge density over time. Nevertheless, it is easy to write down the net charge within any concentric spherical shell of radius, R, using only the current-continuity equation and the divergence theorem:

$$Q(R,t) = Q_0 - 4\pi R^2 J_0 t, \quad E_r(R,t) >> E_\gamma \tag{6}$$

We can then use Gauss's Law and the divergence theorem to conclude,

$$E_r(R,t) = Q(R,t)/(4\pi\varepsilon_0 R^2) = E_{r0}(R) - J_0 t/\varepsilon_0, \quad E_r(R,t) >> E_\gamma \tag{7}$$

where the initial field distribution has been defined as $E_{r0}(r) = Q_0/(4\pi\varepsilon_0 r^2)$.

Notice that (7) is essentially identical to (5) -- even in this very different geometry the field decays linearly everywhere (subject to the high-field limit) at exactly the same rate as before! It is easy to show that the same is also true in a cylindrically symmetric cloud with a uniform charge linear density embedded on its axis. Unfortunately, superposition does not apply to these simple, one-dimensional solutions because of the non-linear behavior of the medium in the high-field limit: Although the current density is in the same direction as the electric field, its magnitude is saturated. [In vector notation, $\boldsymbol{J}(\boldsymbol{r},t) = J_0\boldsymbol{E}(\boldsymbol{r},t)/|\boldsymbol{E}(\boldsymbol{r},t)|$, which is not a linear function of $\boldsymbol{E}$.] The best that we can do toward generalization of the model is to allow the cloud charge distribution in each of these three one-dimensional geometries to depend on the dimension in question. Thus, for example, any concentric, spherically symmetric charge distribution is acceptable in the spherical cloud.

CONCLUSIONS

In summary, a simple model is developed that describes the decay of electric field in a cloud with one-dimensional geometry. A "high-field limit" is defined in which the field decay is linear with time and can be quite slow in comparison not only to that in clear air at the same altitude but also to that in the diffusively reduced conductivity at low field intensities in the same cloud. An example is computed, showing that it can take more than 1½ hours for the field to decay from 50 kV/m to near zero in a realistic thunderstorm anvil.

ACKNOWLEDGEMENTS: The authors acknowledge E. Philip Krider for helpful discussions and the other members of the ABFM Team for essential data. John R. Fields helped clarify the extent to which the high-field limit can be generalized. This work was supported by NASA contract CC-90233B.

REFERENCES

Dye, J.E., W.D. Hall, S. Lewis, E. Defer, G. Dix, J.C. Willett, C.A. Grainger, P. Willis, M. Bateman, D. Mach, H. Christian, and F.J. Merceret, Microphysical Properties and the Decay of Electric Fields in Florida Anvils, presented at the AGU Fall Annual Meeting, San Fransisco, CA, Dec., 2002.

Dye, J.E., J.C. Willett, W.D. Hall, E. Defer, S. Lewis, D. Mach, M. Bateman, H. Christian, C.A. Grainger, P. Willis, and F.J. Merceret, The Decay of Electric Field in Anvils: Observations and Comparison with Model Calculations, this conference.

Klett, J.D., Ion transport to cloud droplets by diffusion and conduction, and the resulting droplet charge distribution, *J. Atmos. Sci., 28*, 78-85, 1971.

Krehbiel, P., Conductivity of clouds in the presence of electric fields, unpublished manuscript, NMIMT, September 14, 1967.

Marshall, T.C., W.D. Rust, W.P. Winn, and K.E. Gilbert, Electrical structure in two thunderstorm anvil clouds, *J. Geophys. Res., 94*, 2171-2181, 1989.

Pruppacher, H.R., and J.D. Klett, *Microphysics of Clouds and Precipitation*, D. Reidel Publishing Company, Dordrecht:Holland, 1978.